Discussion. La Fig. 1 donne une projection de la structure parallèlement à l'axe c. Le Tableau 1* donne les valeurs des coordonnées atomiques et les facteurs d'agitation thermique isotrope équivalents des atomes. Dans le Tableau 2 ont été relevées toutes les distances soufre–métal.

Les quatre atomes de bismuth de l'unité asymétrique sont entourés chacun de six atomes soufre formant des octaèdres très déformés. Les distances Bi–S sont comprises entre 2,53 et 3,63 Å. Cet environnement est habituel pour les dérivés du bismuth. Les deux atomes d'europium de l'unité asymétrique possèdent une coordinence huit. Leur environnement est un prisme à base triangulaire, constitué par trois atomes de soufre ($z = \frac{3}{4}$) et leurs trois homologues ($z = -\frac{1}{4}$). Dans le plan équatorial du prisme contenant l'europium ($z = \frac{1}{4}$) se trouvent deux atomes de soufre qui forment avec lui des liaisons approximativement normales aux faces latérales du prisme. Les distances Eu–S sont comprises entre 3,02 et 3,26 Å. Cet environnement prismatique triangulaire est habituel pour les dérivés de l'europium. Les distances mesurées sont caractéristiques de l'europium divalent. Les octaèdres BiS₆ forment un arrangement compact, entourant les six prismes EuS₈ disposés autour de l'axe 3. Cet arrangement laisse apparaître de larges tunnels autour de l'axe 6. Ces tunnels sont à moitié occupés par des atomes d'europium en position statistique $\frac{1}{2}$. Dans un même tunnel, la distance de 2,04 Å qui sépare deux sites contigus entraîne un arrangement ordonné des atomes d'europium le long d'un même axe c. Ainsi suivant l'axe considéré, les atomes d'europium seront tous soit à la cote $00\frac{1}{4}$, soit à la cote $00\frac{3}{4}$. Ceci est d'ailleurs confirmé par l'observation de traînées de diffusion dans les plans perpendiculaires à l'axe c. Le fait de placer un demi atome d'europium sur le site 2(a) conduit à la formule Eu₁,₁Bi₂S₄ en parfait accord avec l'analyse du composé faite par la microsonde de Castaing. Cet excès d'europium introduit un supplément de charges positives à l'intérieur d'un squelette neutre de formule EuBi₂S₄. Cet exemple de tunnel semi-métallique à l'intérieur d'un réseau tridimensionnel peu conducteur est confirmé par des mesures de conductibilité électrique qui indiquent une conductivité monodimensionnelle très marquée dans la direction de l'axe c. Ce résultat semblerait différent de celui trouvé dans la structure de BaBi₂S₄ (Bengt, 1983) dont les positions atomiques sont similaires à celles de Eu₁,₁Bi₂S₄ mais où les auteurs pensent que le composé est neutre électriquement, la compensation des charges se faisant par un déficit sur les atomes de bismuth.

* Les listes des facteurs de structure et des paramètres thermiques anisotropes ont été déposées au dépôt d'archives de la British Library Lending Division (Supplementary Publication No. SUP 42571: 9 pp.). On peut en obtenir des copies en s'adressant à: The Executive Secretary, International Union of Crystallography, 5 Abbey Square, Chester CH1 2HU, Angleterre.

Références

BECKER, P. & COPPENS, P. (1975). *Acta Cryst.* A31, 417–425.
BENGT, A. (1983). *Acta Chem. Scand. Ser. A*, 37, 399–407.
BUSING, W. R. (1971). *Acta Cryst.* A27, 683–684.
GERMAIN, G. & WOOLFSON, M. M. (1968). *Acta Cryst.* B24, 91–96.
International Tables for X-ray Crystallography (1974). Tome IV, pp. 71–78. Birmingham: Kynoch Press. (Distributeur actuel D. Reidel, Dordrecht.)
LEMOINE, P., CARRÉ, D. & GUITTARD, M. (1982). *Acta Cryst.* B38, 727–729.
MEULENAER, J. DE & TOMPA, H. (1965). *Acta Cryst.* 19, 1014–1018.

Zr₂₁Re₂₅, a New Rhombohedral Structure Type Containing 12 Å-Thick Infinite MgZn₂(Laves)-Type Columns

By K. Cenzual and E. Parthé

Laboratoire de Cristallographie aux Rayons X, Université de Genève, 24 quai Ernest Ansermet, CH-1211 Genève 4, Switzerland

and R. M. Waterstrat

American Dental Association, National Bureau of Standards, Gaithersburg, MD 20899, USA

Abstract. Zr₂₁Re₂₅, $M_r = 6570.6$, $hR276$, $R\bar{3}c$, $a = 25.847$ (1), $c = 8.771$ (1) Å, $V = 5074.7$ (6) Å³, $Z = 6$, $D_x = 12.9$ Mg m⁻³, Mo $K\alpha$, $\lambda = 0.71069$ Å, $\mu = 100.0$ mm⁻¹, $F(000) = 16\,290$, $T = 293$ K, $wR = 0.068$ for 1045 independent reflections. Hf₂₁Re₂₅ [$a = 25.773$ (4), $c = 8.760$ (2) Å] and Ti₂₁Mn₂₅ [a

$= 23\cdot596$ (11), $c = 8\cdot035$ (6) Å] crystallize with the same structure type. The Zr$_{21}$Re$_{25}$ structure is characterized by large segments (204 of the 276 atoms in the unit cell) of hexagonal MgZn$_2$ (Laves) type, a structure type found with neighbouring ZrRe$_2$ (HfRe$_2$ or TiMn$_2$).

Introduction. Three compounds, formed by peritectic reactions, have been reported in the Zr–Re phase diagram (Savitskii, Tylkina & Tsiganova, 1961). ZrRe$_2$ adopts the hexagonal MgZn$_2$ (Laves) type, while Zr$_5$Re$_{24}$ crystallizes with the Ti$_5$Re$_{24}$ type (Trzebiatowski & Niemiec, 1955), a binary ordering variant of the α-Mn type. The third compound was found at the approximate stoichiometry 2:1 and Savitskii and coworkers reported it to be isotypic with the σ phase.

A hexagonal Laves phase and a cubic Ti$_5$Re$_{24}$-type phase were also identified in the Hf–Re phase diagram, determined by Taylor, Kagle & Doyle (1963). These authors further observed a phase of unknown structure, called (Hf,Re)φ, near the equiatomic composition, which they tentatively indexed with a tetragonal cell of $a = 8\cdot90$, $c = 13\cdot89$ Å. Savitskii & Tylkina (1962), on the other hand, reported an Hf–Re phase diagram analogous to the Zr–Re diagram containing a tetragonal σ-phase-type compound at the approximate stoichiometry Hf$_2$Re. In preliminary results one of us (Waterstrat, 1984) confirmed from a comparison of Guinier films that the phases called Zr$_2$Re and (Hf, Re)φ (or 'Hf$_2$Re') are isotypic,* but concluded that they were probably not of the σ type.

A phase isotypic with (Hf,Re)φ had also been found in the system Ti–Mn at approximately 50·5 at.% Mn by Waterstrat, Das & Beck (1962). In analogy with the cell reported for (Hf,Re)φ, the (Ti,Mn)φ phase had also been tentatively indexed with a tetragonal cell with $a = 8\cdot19$ and $c = 12\cdot81$ Å. It seemed of interest to determine the crystal structure of these isotypic phases.

An interesting approach to the often complicated task of describing intermetallic structures appears to be the analysis of the atom arrangement as an intergrowth of different structure segments, characteristic of simple alloy structure types (see for example Kripyakevich, 1971; Kripyakevich & Grin', 1978; Andersson & Hyde, 1982; Andersson, 1983; Parthé, Chabot & Cenzual, 1985). It should be interesting to see if this concept, which has proved its usefulness for the description of a large number of structures found among binary and ternary alloys, could be applied also to this structure type.

Experimental. Sample of nominal composition Zr$_2$Re, containing mainly the 'Zr$_2$Re' phase together with some β-Zr, prepared in an arc furnace. It was further suspended with Re wire and annealed at 1943 K for 2 h. One needle-shaped crystal (95 × 25 × 25 μm), which had formed near the wire, mounted on automatic four-circle diffractometer (Philips PW 1100). Cell parameters obtained by least-squares refinement of 2θ values of 18 reflections ($32 \le 2\theta \le 60°$), Mo $K\alpha_1$ radiation, program *FINAX* (Hovestreydt, 1983). Conditions for reflections, $-h+k+l = 3n$ and $l = 2n$ for $h0l$ and symmetry-equivalent reflections in Laue group $\bar{3}m1$, led to possible space groups $R\bar{3}c$ and $R3c$. 1837 unique reflections ($0 \le h, k \le 36$; $l \le 12$, including 101 systematic extinctions) and their antireflections ($R_{int} = 3\cdot9\%$); $0\cdot077 \le \sin\theta/\lambda \le 0\cdot703$ Å^{-1}; ω–2θ scan mode; two reference reflections: $9\bar{8}2$ and $11,\bar{5},1$ (max. intensity variation ±2·5%); spherical absorption correction ($\mu R = 2\cdot385$, $13\cdot3 \le A^* \le 21\cdot0$). Structure solved by direct methods in centrosymmetric space group $R\bar{3}c$ using *MULTAN*80 (Main, Fiske, Hull, Lessinger, Germain, Declercq & Woolfson, 1980), programs from *XRAY*76 system (Stewart, Machin, Dickinson, Ammon, Heck & Flack, 1976) used for data reduction and structure refinements. Sites occupied by Re recognized from displacement parameters of the sites and from crystallochemical arguments (no interatomic distances $\le 2\cdot90$ Å between Zr atoms). Full-matrix refinement of 32 parameters (scale factor, 21 atomic positional and 10 isotropic displacement parameters) from F values of 1050 independent reflections, of which 663 considered observed $[I \ge 3\sigma(I)]$ plus 387 with $I < 3\sigma(I)$ but calculated values greater than observed, down to $R = 8\cdot3\%$. R further lowered to 6·8% by applying a weighting scheme $[w = 1/\sigma^2(F_{obs})]$ and by ignoring reflections 802 and 18,0,0 ($S = 2\cdot11$; $-15\cdot1 \le$ residual electron density $\le 17\cdot2$ e Å^{-3}; shift/e.s.d. in last cycle $\le 0\cdot0002$).† Atomic scattering factors for neutral atoms and anomalous-dispersion corrections from *International Tables for X-ray Crystallography* (1974).

The composition determined from X-ray data, 45·7 at.% Zr–54·3 at.% Re, is slightly outside the homogeneity ranges indicated by Waterstrat, Das & Beck (1962) for the isotypic (Ti,Re)φ phase or by Taylor, Kagle & Doyle (1963) for the isotypic φ phase in the Hf–Re system, but relatively far away from the approximate stoichiometry Zr$_2$Re (Savitskii, Tylkina & Tsiganova, 1961). However, the calculated powder diagram of Zr$_{21}$Re$_{25}$, using *LAZY PULVERIX* (Yvon,

---

* A phase containing 70 at.% Zr–30 at.% Os was reported to be isotypic with (Hf,Re)φ (Brewer & Wengert, 1973). However, Eremenko, Semenova & Shtepa (1976), who studied the Zr–Os phase diagram, only observed, in this composition range, a phase of stoichiometry 11:4, later identified as being isotypic with cubic Sc$_{11}$Ir$_4$ (Chabot, Cenzual & Parthé, 1980).

Jeitschko & Parthé, 1977), is in good agreement with the intensities, observed on a Guinier film, of the majority phase in the sample of nominal composition Zr_2Re. Moreover, the atomic displacement parameters do not indicate any significant vacancies nor does the difference electron density map show any residual peaks.

In order to check for the isotypy of the $(Hf,Re)\varphi$ phase a sample of composition $Hf_{21}Re_{25}$ was prepared in an arc furnace under Ar atmosphere. A Guinier film of the unannealed sample showed lines from rhombohedral $Hf_{21}Re_{25}$ and hexagonal $HfRe_2$. The cell parameters of $Hf_{21}Re_{25}$, given in the *Abstract,* were refined, using the program *FINAX* (Hovestreydt, 1983), from the 2θ values of 17 reflections [$32 \le 2\theta \le 53°$, Cu $K\alpha$ ($\lambda = 1.54180$ Å), internal Si standard ($a = 5.4307$ Å)].

In the case of $(Ti, Mn)\varphi$ an X-ray powder diffraction pattern measured with a Debye–Scherrer camera using Fe $K\alpha$ radiation was published by Waterstrat, Das & Beck (1962). The sample had a nominal composition 50·15 at.% Mn–49·85 at.% Ti and contained some β-Ti. It had been homogenized for 2 months at 1173 K. There is good agreement between the observed relative intensities (estimated on a six-grade scale between strong and very weak) and those calculated for $Ti_{21}Mn_{25}$ with $Zr_{21}Re_{25}$ type using the powder-diagram-simulation program *LAZY PULVERIX* (Yvon,

Jeitschko & Parthé, 1977). The cell parameters (see *Abstract*) were refined (program *FINAX*) from the 2θ values of ten reflections in the region 45–60°.

Discussion. In Table 1 are listed atomic positional and isotropic displacement parameters of the ten atom sites in $Zr_{21}Re_{25}$. Interatomic distances up to 4 Å have been calculated and deposited. In Table 2 are shown the coordinations of the different atom sites by indicating the number of atoms of each kind at a distance shorter than 4 Å and the relative differences (Δ) between the observed distances (d) and the sum of the radii (r) of

Table 1. *Atomic positional and isotropic displacement parameters for* $Zr_{21}Re_{25}$ *with space group* $R\bar{3}c$

The temperature factor is expressed as $T = \exp[-2\pi^2 U(2\sin\theta/\lambda)^2]$.

E.s.d.'s are given in parentheses.

		x	y	z	$100U(\text{Å}^2)$
Zr(1)	36(f)	0·0021 (3)	0·2306 (3)	0·0424 (8)	0·7 (1)
Re(1)	36(f)	0·0582 (1)	0·1778 (1)	0·2480 (4)	0·9 (1)
Zr(2)	36(f)	0·1161 (4)	0·1164 (3)	0·0659 (7)	0·9 (1)
Re(2)	36(f)	0·2342 (1)	0·1754 (1)	0·2477 (4)	0·8 (1)
Re(3)	36(f)	0·2350 (1)	0·1163 (1)	0·0000 (4)	0·8 (1)
Zr(3)	36(f)	0·3129 (3)	0·1084 (3)	0·2481 (9)	1·1 (2)
Re(4)	18(e)	0·0610 (2)	0	$\frac{1}{4}$	1·0 (1)
Re(5)	18(e)	0·4446 (2)	0	$\frac{1}{4}$	0·7 (1)
Zr(4)	18(e)	0·6943 (4)	0	$\frac{1}{4}$	1·3 (2)
Re(6)	6(b)	0	0	0	1·0 (1)

Table 2. *The number and kind of neighbours out to 4 Å of the atom sites in* $Zr_{21}Re_{25}$ *and the relative differences* (Δ) *between the observed interatomic distances* (d) *and the sum of atomic radii for 12-coordinated atoms* ($\sum r$), *calculated according to the formula* $\Delta = 100(d-\sum r)/\sum r$

Atomic radii used for Zr and Re are 1·602 and 1·375 Å respectively (Teatum, Gschneidner & Waber, 1960).

	Zr(1)	Zr(2)	Zr(3)	Zr(4)	Re(1)	Re(2)	Re(3)	Re(4)	Re(5)	Re(6)
Zr(1)	+13·7	−3·9	−3·2 −1·6 +6·7	2(−2·3) 2(+0·9)	+1·9 +3·9	−2·1 +0·5	+0·2 +0·8		2(+1·9)	
Zr(2)	−3·9	+0·5 2(+0·8)			+4·6 +5·5 +6·2 +7·1	+3·7 +4·2	+3·7 +5·1	2(+2·8) 2(+3·0) 2(+4·7)		6(+2·8)
Zr(3)	−3·2 −1·6 +6·7		−6·1 −3·4	2(+1·5)	+2·6	+2·2 +9·7 +3·8	+2·1 +2·2		2(−0·9) 2(+3·8)	
Zr(4)	−2·3 +0·9		+1·5	2(−0·9)		−1·8			2(0·0)	
Re(1)	+1·9 +3·9	+4·6 +5·5 +6·2 +7·1	+2·6		−5·2	−4·6	−3·4 −3·1	2(−4·9)		
Re(2)	−2·1 +0·5	+3·7 +4·2	+2·2 +9·7	2(−1·8)	−4·6	−4·3	−3·3 −3·2		2(−2·9)	
Re(3)	+0·2 +0·8	+3·7 +5·1	+2·1 +2·2 +3·8		−3·4 −3·1	−3·3 −3·2			2(−1·5)	
Re(4)		+2·8 +3·0 +4·7			−4·9			2(−0·7)		6(−1·8)
Re(5)	+1·9		−0·9 +3·8	2(0·0)		−2·9	−1·5	2(−1·8)		
Re(6)		+2·8						2(−1·8)		
$\sum$	14	16	14	12	12	12	12	12	12	12

12-coordinated atoms (Teatum, Gschneidner & Waber, 1960), expressed in per cent according to the formula $\Delta = 100(d-\sum r)/\sum r$. The minimum distance observed between Zr and Re is 2·915 (8) Å [Zr(1)–Re(2), $\Delta = -2\cdot1$], while no distances shorter than 2·608 (4) Å [Re(1)–Re(1), $\Delta = -5\cdot2$] and 3·008 (12) Å [Zr(3)–Zr(3), $\Delta = -6\cdot1$], respectively, occur between atoms of one kind. All sites occupied by Re atoms, as well as Zr(4), are 12-coordinated, whereas Zr(1) and Zr(3) have 14 atoms at distances shorter than 4 Å. Zr(2) is surrounded by 12 Re and 4 Zr atoms forming a Friauf polyhedron, i.e. a truncated tetrahedron of Re, the four hexagonal faces of which are capped by Zr atoms.

Friauf polyhedra are found in a great number of intermetallic structure types (Samson, 1968), including among these the commonly appearing Friauf or Laves phases. The $MgCu_2$, $MgZn_2$ and other Laves-phase stacking variants can be described as three-dimensional arrangements of interpenetrating Friauf polyhedra where the truncated tetrahedra, formed by the smaller majority atoms and centred by the larger minority atoms, share hexagonal faces. In $Zr_{21}Re_{25}$ the Friauf polyhedra, centred by Zr(2), are arranged in infinite columns parallel to the c axis; part of two of these can be seen in Fig. 1. The sites at the vertices of the truncated tetrahedra are occupied by the smaller Re atoms. Of the Zr atoms only the Zr(1) atoms, located above the outer hexagonal faces and completing the Friauf polyhedra (but having themselves a different coordination), are shown. It can be seen from the cross section of the column to the left that the truncated tetrahedra of six Friauf polyhedra (three with hexagonal and three with triangular faces at the interface) form part of a close-packed layer of polyhedra, similar to those found in the Laves phases. These finite slabs are then stacked upon each other with mirror planes at the interfaces, in the same way as in $MgZn_2$, forming 12 Å-thick infinite columns parallel to the c axis.

The atom arrangement in one column is shown in detail in a projection along [001] in Fig. 2(b). A large circle, drawn with a plain line, delimits one of the columns described above. These Laves-type columns
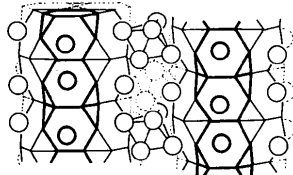
account for seven of the ten atom sites in the structure [Zr(1) and Zr(2), Re(1), Re(2), Re(3), Re(4) and Re(6)], i.e. 204 of the 276 atoms in the unit cell. The coordinates of these sites differ very little from those that can be calculated from the coordinates of the atoms in the $MgZn_2$ type, found with the neighbouring $ZrRe_2$ (or $HfRe_2$) and shown in a similar projection along [001] in the upper part of Fig. 2. It can further be seen by comparing Figs. 2(a) and 2(b) that the atoms in $Zr_{21}Re_{25}$, which are outside the circle drawn with a plain line but inside that drawn with a dashed line, are at sites that are not far from those observed in the $ZrRe_2$ structure [circles of corresponding diameters have been drawn in Fig. 2(a)], but that some sites that in $ZrRe_2$ are occupied by Re atoms are here occupied by Zr atoms and vice versa. It seems difficult to associate the atom arrangement in this 'transition region' with any of the known simple structure types. In agreement with the rhombohedral symmetry there are three symmetry-related columns in the structure, centred around [00z], $[\frac{1}{3} \frac{2}{3} z]$ and $[\frac{2}{3} \frac{1}{3} z]$ respectively,
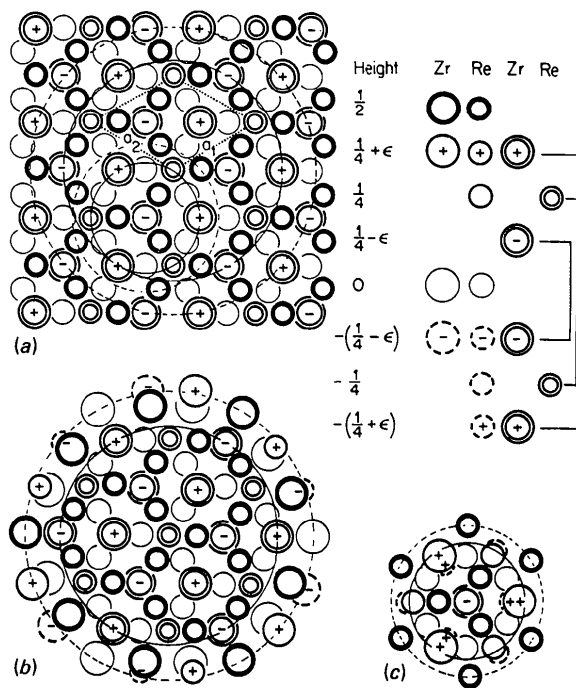
Fig. 2. (a) $Zr(Hf)Re_2$ ($MgZn_2$ type) and $MgZn_2$-type columns observed in (b) $Zr(Hf)_{21}Re_{25}$ and (c) $Zr(Hf)_5Re_{24}$ (Ti_5Re_{24} type) in projections along [001] of the (triple) hexagonal cells. Heights of the atoms are indicated on a relative scale, the parameter ϵ takes values between 0·04 and 0·08. Large circles drawn with plain lines in (b) and (c) delimit the part of the columns where little deviation from the $MgZn_2$ type is observed, while the domain between the inner circle and the outer circle, drawn with a dashed line, corresponds to the transition region. Circles of corresponding diameter have been drawn on the projection of $ZrRe_2$ in order to simplify the comparison.

Fig. 1. Part of two infinite Laves-type columns found around [00z] and $[\frac{1}{3}\frac{2}{3}z]$ in $Zr_{21}Re_{25}$ represented by face-joined truncated tetrahedra [formed in the structure by Re(1,2,3,4,6) atoms and centred by Zr(2) atoms]. The open circles above the hexagonal faces of the truncated tetrahedra correspond to the Zr(1) atoms, which complete the Friauf polyhedra. These Zr atoms together with Zr(3) and Zr(4) atoms in the transition region form distorted octahedra centred by Re(5) (not shown, total coordination 12).

and shifted by $c/3$ with respect to each other. The relative arrangement of these columns within the unit cell along [001] can be seen in the upper part of Fig. 3 where the circles (plain and dashed lines) correspond to the large circles, drawn on a different scale, in Fig. 2(b).

The structure of the third phase in the Re-rich part of the Zr–Re (and Hf–Re) system, Zr_5Re_{24} (Hf_5Re_{24}) with cubic Ti_5Re_{24} type, an ordering variant of α-Mn, can also be related to the $MgZn_2$-type structure. Laves-type columns may be considered parallel to the cube diagonals. It can be seen in Fig. 2(c), showing the atom arrangement of one of these in a projection along [111] of the cubic unit cell, that their diameter only corresponds to one Friauf polyhedron and that the Friauf polyhedron surrounding each second Zr atom on the column axis is composed of one Zr and 15 Re atoms instead of four Zr and 12 Re atoms. The relative arrangement of the columns in the corresponding triple hexagonal cell and their size, compared with the columns found in $Zr_{21}Re_{25}$, are shown in the lower part of Fig. 3. If the intersecting columns parallel to the different cube diagonals are combined, the structure may be considered as a three-dimensional arrangement where each regular Friauf polyhedron (centred at the Bravais points) is tetrahedrally surrounded by four pseudo-Friauf polyhedra.

The formation of Friauf polyhedra as a characteristic structural feature seems to apply also to the system Ti–Mn. According to Waterstrat, Das & Beck (1962), only three intermetallic phases are stable in this system

below 1200 K: $Ti_{21}Mn_{25}$, $(Ti,Mn)\rho$ and $TiMn_2$ with hexagonal Laves-phase type. The ordered Ti_5Re_{24} type does not form but the α-Mn structure has a large solubility for Ti. It seems reasonable to expect that the still unknown structure of $(Ti,Mn)\rho$, which appears at an intermediate composition between $Ti_{21}Mn_{25}$ and $TiMn_2$, also contains Friauf polyhedra.

A large number of other structure types found with interatomic compounds have been described using Laves-type segments, often combined with segments derived from the $CaCu_5$, Zr_4Al_3 or Cr_3Si types (see, for example, Parthé & Lemaire, 1975; Kripyakevich & Yarmolyuk, 1977; Andersson, 1977; Parthé, Chabot & Cenzual, 1985). However, where Laves-type columns occur in these structure types these are cut parallel to the [110] direction of $MgZn_2$.

Fig. 3. Arrangement of the Laves-type columns in the triple hexagonal unit cells of (a) rhombohedral $Zr(Hf)_{21}Re_{25}$ and (b) cubic $Zr(Hf)_5Re_{24}$ in projections along [001]. Circles drawn with plain or dashed lines correspond to the large circles, drawn with a different scale, in Figs. 2(b) and 2(c), where the atom arrangement in one column can be studied in detail. Inside the circles are indicated the relative shifts of the atomic coordinates in the c direction of the hexagonal cells.

References

ANDERSSON, S. (1977). *J. Solid State Chem.* **23**, 191–204.
ANDERSSON, S. (1983). *Angew. Chem. Int. Ed. Engl.* **22**, 69–81.
ANDERSSON, S. & HYDE, B. G. (1982). *Z. Kristallogr.* **158**, 119–131.
BREWER, L. & WENGERT, P. R. (1973). *Metall. Trans.* **4**, 83–104.
BROWN, I. D. (1983). *Acta Cryst.* A**39**, 216–224.
CHABOT, B., CENZUAL, K. & PARTHÉ, E. (1980). *Acta Cryst.* B**36**, 7–11.
EREMENKO, V. N., SEMENOVA, E. L. & SHTEPA, T. D. (1976). *Dopov. Akad. Nauk Ukr. RSR Ser. A*, pp. 661–665.
HOVESTREYDT, E. (1983). *J. Appl. Cryst.* **16**, 651–653.
International Tables for X-ray Crystallography (1974). Vol. IV. Birmingham: Kynoch Press. (Present distributor D. Reidel, Dordrecht.)
KRIPYAKEVICH, P. I. (1971). *Sov. Phys. Crystallogr.* **15**, 596–601.
KRIPYAKEVICH, P. I. & GRIN', YU. N. (1978). *Sov. Phys. Crystallogr.* **23**, 45–49.
KRIPYAKEVICH, P. I. & YARMOLYUK, YA. P. (1977). *Theoretical and Experimental Chemistry (USSR)*. *Vestn. L'vovsk Univ. Ser. Khim.* **19**, 3–9.
MAIN, P., FISKE, S. J., HULL, S. E., LESSINGER, L., GERMAIN, G., DECLERCQ, J.-P. & WOOLFSON, M. M. (1980). *MULTAN80. A System of Computer Programs for the Automatic Solution of Crystal Structures from X-ray Diffraction Data*. Univs. of York, England, and Louvain, Belgium.
PARTHÉ, E., CHABOT, B. & CENZUAL, K. (1985). *Chimia*, **39**, 164–174.
PARTHÉ, E. & LEMAIRE, R. (1975). *Acta Cryst.* B**31**, 1879–1889.
SAMSON, S. (1968). In *Structural Chemistry and Molecular Biology*, edited by A. RICH & N. DAVIDSON, pp. 687–717. San Francisco: W. H. Freeman.
SAVITSKII, E. M. & TYLKINA, M. A. (1962). In *Rhenium*, pp. 67–83. New York: Elsevier.
SAVITSKII, E. M., TYLKINA, M. A. & TSIGANOVA, I. A. (1961). *Sov. J. At. En.* **7**, 724–727.
STEWART, J. M., MACHIN, P. A., DICKINSON, C. W., AMMON, H. L., HECK, H. & FLACK, H. (1976). The *XRAY76* system. Tech. Rep. TR-446. Computer Science Center, Univ. of Maryland, College Park, Maryland.
TAYLOR, A., KAGLE, B. J. & DOYLE, N. J. (1963). *J. Less-Common Met.* **5**, 26–40.
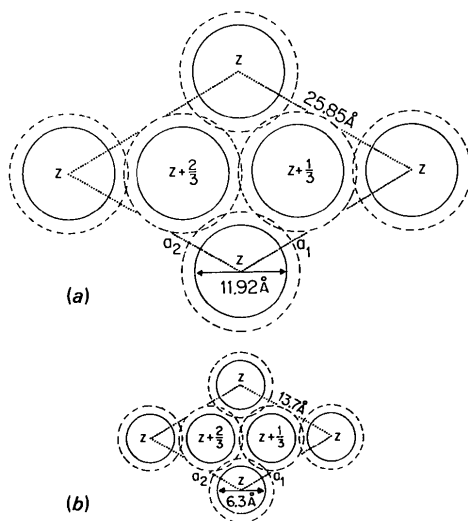
TEATUM, E., GSCHNEIDNER, K. JR & WABER, J. (1960). Cited in *The Crystal Chemistry and Physics of Metals and Alloys* (1972), edited by W. B. PEARSON, p. 151. New York: John Wiley.

TRZEBIATOWSKI, W. & NIEMIEC, J. (1955). *Rocz. Chem.* **29**, 277–283.

WATERSTRAT, R. M. (1984). Unpublished results.

WATERSTRAT, R. M., DAS, B. N. & BECK, P. A. (1962). *Trans. Metall. Soc. AIME*, **224**, 512–518.

YVON, K., JEITSCHKO, W. & PARTHÉ, E. (1977). *J. Appl. Cryst.* **10**, 73–74.

Hexabarium Titanium(IV) Tetraniobate(V); a Rietveld Refinement of Neutron Powder Diffraction Data

BY H. C. VAN DUIVENBODEN, H. W. ZANDBERGEN AND D. J. W. IJDO

Gorlaeus Laboratories, State University, Leiden, PO Box 9502, 2300 RA Leiden, The Netherlands

Abstract. $Ba_6TiNb_4O_{18}$, $M_r = 1531 \cdot 6$, rhombohedral, $R\bar{3}m$, $a = 5 \cdot 7852$ (1), $c = 42 \cdot 4886 \cdot (3)$ Å, $V = 1231 \cdot 52$ (2) Å^3, $Z = 3$, $D_x = 6 \cdot 195$ (1) Mg m^{-3}, room temperature. The structure has been refined by Rietveld analysis of powder neutron diffraction data ($\lambda = 1 \cdot 909$ Å, $R_{wp} = 7 \cdot 80\%$) for 216 reflections. The structure is of rhombohedral 18L type. BaO$_3$ layers are stacked $(hhcccc)_3$, resulting in a perovskite lattice with a shear plane every sixth layer. In the shear plane the octahedra are not filled. Ti and Nb ions have an octahedral coordination of oxygen atoms, and the octahedra share corners.

Introduction. The preparation, crystal structure determination and solubility test in water at elevated temperatures and pressures form part of a research program to investigate compounds with perovskite or related structures for their properties as a host lattice for nuclear waste. $Ba_6TiNb_4O_{18}$ was reported to adopt a rhombohedral 18L lattice (Schittenhelm & Kemmler-Sack, 1980), but the structure was not solved.

Experimental. AR starting materials $BaCO_3$, TiO_2 and Nb_2O_5 thoroughly mixed in an agate mortar in the appropriate ratio; mixture heated in Al_2O_3 crucible at 1270 K for 1 d and after grinding product was sealed in a platinum capsule and heated at 1570 K for one week.

X-ray powder diffraction pattern obtained with Philips PW 1050 diffractometer; all lines indexed with rhombohedral unit cell; in accordance with electron diffraction data (Siemens Elmiskop 102 electron microscope, double tilt, lift cartridge, 100 kV). Since no single crystals available, Rietveld's (1969) method used for refinement of neutron powder diffraction data; neutron powder profile recorded (293 K, atmospheric pressure) on D1A diffractometer of the Institut Laue–Langevin in Grenoble; $6 < 2\theta < 157 \cdot 9°$ in steps of 0·05°; sample (25 g) contained in thin-walled vanadium can (⌀ 18 mm); neutron wavelength 1·909 Å. No precautions to avoid preferred orientation. No absorption correction. Background determined by extrapolation between those parts in diagram containing no contribution or, for higher values of 2θ, only a small contribution from reflections. The stability in water and 10% NaCl solution at 573 K and 0·2 GPa for 1 week was tested: $Ba_6TiNb_4O_{18}$ was stable under these conditions. Trial model was deduced from known structure of $Ba_5\square Ta_4O_{15}$ ($hhccc$). This structure is built up from BaO$_3$ layers with Ta ions between them, but vacancies between the hh layers. In the trial model the $hhccc$ stacking of $Ba_5\square Ta_4O_{15}$ is combined with a sixth layer giving the rhombohedral $(hhcccc)_3$ structure, space group $R\bar{3}m$ (No. 166): Ba(1), Ba(2), Ba(3), Nb(1), Nb(2) on 6(c) sites; Ti on 3(b) site; O(1), O(2) and O(3) on 18(h) sites. 30 parameters in refinement: a scale factor, three halfwidth parameters defining Gaussian-like shape of reflections, counter zero error, preferred-orientation parameter (along [001]), unit-cell parameters, atomic positional parameters, isotropic thermal parameters, asymmetry parameter and three occupation numbers with a constraint forcing the formula to $Ba_3TiNb_4O_{18}$. In the final refinement it was necessary to introduce Ti and Nb on the octahedral positions. No significant occupation was found at the octahedral position at 0,0,0. Coherent scattering lengths: Ba 5·25, Ti −3·438, Nb 7·054, O 5·805 fm (Koester, Rauch, Herkens & Schroeder, 1981). The Rietveld (1969) program minimizes the function $\chi^2 = \sum_i w_i [y_i(\text{obs.}) - (1/c)y_i(\text{calc.})]^2$, where $y_i(\text{obs.})$ and $y_i(\text{calc.})$ are observed and calculated data points, w_i is statistical weight $[1/y_i(\text{obs.})]$ allotted to each data point and c is the scale factor; $R_{wp} = 100[\sum w_i | y_i(\text{obs.}) - (1/c)y_i(\text{calc.}) |^2/\sum w_i | y_i(\text{obs.}) |^2]^{1/2} = 7 \cdot 80\%$, compared with 7·65% expected on purely statistical grounds.